Using Remote Sensing to Assess Fire Severity and Vegetation Regeneration

Chukwuemeka Fortune Igwe [1], and Edwige Mukundane[2]
NOVA Information Management School
Campus de Campolide, 1070-312 Lisboa, Portugal
Tel.: + 351 21 382 8610; Fax: + 351 21 382 8611 john@gsupt.org; susanne@ gsupt.org

Residencia
Av. Liberdade n.º 6, 1200-123 Lisboa, Portugal
Tel.: + 351914850512, +351914851707
m20190646@novaims.unl.pt; m20190649@novaims.unl.pt

Abstract

Wildfires continue to occur in most terrestrial ecosystems resulting in various social, economic, and environmental costs to world economies. Appropriate assessment of ecosystems and biodiversity affected by fire epidemics is crucial to modelling and forecasting post-fire activities for managing and recovery of affected areas. Earth observation measurements have been identified as effective and efficient tools for assessing, monitoring, and predicting wildfires, as well as getting a better understanding of how forest ecosystems respond to them. Remotely sensed Landsat 8 multi-spectral satellite data with spatial 30m resolution is utilized in this study to obtain spectral indices and supervised classification that is used to assess burn severity extent and post-fire vegetation recovery. Besides the conventional maximum likelihood classifier, the differenced Normalised Burn Ratio (dNBR) derived from the difference between pre-fire NBR and post-fire NBR, Normalized Difference Vegetation Index NDVI and Geographical Information System (GIS) was applied to analyze fire impact for a post-fire occurrence period of nine months. This study highlights results obtained from both supervised classification and spectral indices, showing deficiencies in the use of the current approach while giving an accurate assessment of the results. The results show that using the maximum likelihood was preferable, with an overall accuracy of 86% and kappa statistics of 72%. Finally, it was discovered that the amount of vegetation that regenerated was about 8.86% of the land area (3525.132102) that was consumed by fire.

.Keywords: Remote Sensing, Post-Fire Assessment, fire Severity, Vegetation Regeneration

1 Introduction

Burn Severity is a descriptive term that integrates the various phenomenological characteristics of a fire altered landscape. Wildfires are one of the most disturbance agents causing significant and prolonged impacts to ecosystems and landscapes (Tran et al. 2018). According to the U.S. Fire service, more than 700 wildfires occur every year, burning down approximately 7 million acres of land and destroying more than 26,000 structures. The causes of wildfires can be human factors or natural factors such as lightning or volcanic eruptions. The impact of fires ranges from affecting climate cycles to causing significant alteration land cover structures. Assessment of wildfire impacts is crucial to provide post-fire information for management, treatments, monitoring of affected areas, and planning for vegetation recovery (Bastos et al., 2011). Today earth observations are providing measurements for wildfire occurrences giving information for the understanding of the events on a temporal scale. Wildfires can be remotely sensed using either passive or active sensors with passive data being the most used for deriving spectral indices for studying burn severity (Veraverbeke et al. 2009). Standard spectral indices in

assessing burn severity are computed from combining portions of the Visible, Near InfraRed and Mid -Infrared of the electromagnetic spectrum (Tran et al. 2018). The visible and mid-infrared portions are sensitive to variations in soil colour, mid-infrared for soil composition, and near-infrared for moisture and chlorophyll, which are prime land and vegetation properties that are most affected by the fire. Spectral indices have been tested on various studies related to landscape processes. The potentials of spectral bands especially the red groups and the mid-infrared portions combined to compute Normalised Burn Ratio (NBR) have been tested for fire severity estimation for a range of ecosystems such as Siberian Boreal Larch forest (Thuan Chu et al. 2015) or Mediterranean ecosystems (A. Poly-chronaki A C et al. 2013). where NIR is the reflectance in the Near-infrared and Red is the reflectance in the red band portion of the visible spectrum. The Normalised Burn Ratio (NBR) is computed from;

$$NBR = \frac{NIR\text{-}SWIR}{NIR+SWIR} \quad (1)$$

where

NIR is the reflectance in the Near-infrared, and SWIR is the reflectance in the short-wave infrared.

The differenced Normalised Burn Ratio (dNBR) calculated from the difference between pre and post-fire conditions is a powerful tool used to better understand fire burn extent and severity (Leah Wasser et al. 2017). The Normalised Difference Vegetation Index (NDVI) is also among the most used indices to as-sess burn severity, with the differenced Normalised Difference Vegetation Index (dNDVI) providing a better understanding of bi-temporal approaches to estimating fire severity and postfire vegetation regeneration evaluation (Sander Veraverbeke et al. 2009). NDVI is computed from;

$$NDVI = \frac{(NIR - Red)}{(NIR + Red)} \quad (2)$$

Several approaches have been proposed for post-fire vegetation regeneration assessment with monitoring vegetation recovery from spectral indices being the most used, NDVI is the most common (Thuan Chu et al. 2015). The maximum Likelihood supervised classification method, which is based on the Bayes theorem, has, over time, been used mapping fire damage (Jamaruppin et al. 2018). In as much as several studies have analyzed fire severity and vegetation regeneration using earth observation data, only a few integrate both spectral indices and image classification in a single study (Viana-Soto et al. 2017). The increased integration of both aspects and analyses would improve the predictive models of investigating the factors that determine post-fire regeneration patterns (Viana-Soto et al. 2017). In this paper, using butte county California as a case study, we assess the burn severity using both spectral indices (NBR) and classification techniques. The NDVI is used to provide an evaluation of vegetation recovery in the study area. Accuracy assessment for both image classification and spectral indices is defined by deriving confusion matrix; this provided a comparison between ground truth reference data from google earth imagery and the corresponding results from spectral indices and classification. Also, Post-fire vegetation recovery monitoring was vegetation indices along with supervised

classification. Finally, the burn severity map was produced using the USGS proposed fire severity classification.

1.1 Objectives

The primary objectives of this project were:

1) To Capture the extent of the Burn area as well as the level of severity that existed during the incident using both the differenced normalized burn ratio index (DNBR), normalized difference vegetation index (NDVI) and supervised classification;

2) To extract estimates of vegetation-regenerated by explicitly measuring the spectral signature of the area's satellite imagery and to quantitatively determine the amount of vegetation recovered from the field using NDVI.

2 Study area

The study area is located beside the rural community of Concow and foothill town of Paradise Town, Butte County (known as the “Land of Natural Wealth and Beauty”)in California (Fig. 1), part of the United States of America. The Feather River and Butte Creek enter the county. According to the Köppen Climate Classification System, the area surrounding Paradise has a hot-summer Mediterranean climate (CSA). The Sacramento River is part of the western boundary of the county. The county sits along the Sierra Nevada's western steep slope. The elevation of the area is 1.778 feet (542 m). The town itself is about 8 miles east of Chico City and 10 miles north of Oroville. The city has a total area of 18.3 square miles (47 km2), over 99 percent of its land, according to the U.S. Census Bureau. Most of the soils are well-drained reddish-brown loam, often gravely, and often grading with rising depth to clay loam or asphalt created on volcanic material.

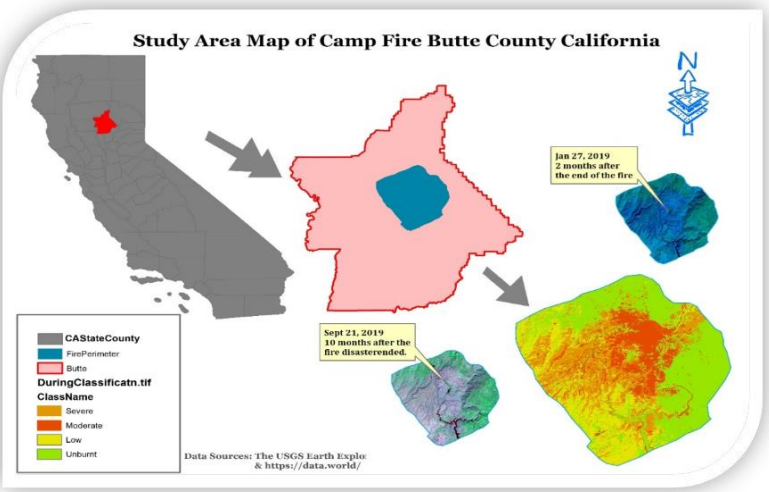

Figure 1 Study area location in Butte County, USA, and the distribution of fire scars (field plot distribution) within the study area. And (Landsat 8 OLI/TIRS C1 level 2 imagery: bands 7:5:4 as the R: G: B combination; Projection WGS 1984 UTM Zone 10N datum.

All these meteorological factors contributed to increasing fire intensity and severity. The fire began on Thursday morning, November 8, 2018, and lasted for about 17 days, killing about 29 people. It almost de-stroyed Paradise City. It now ties with the 1933 Griffith Park Blaze in Los Angeles as the cruelest in the US (Schneising, Buchwitz, Reuter, Bovensmann, & Burrows, 2019). Researchers estimate that 2018 was not only California's worst fire season, but it was also the worst in terms of scope, with more than 1.6 million acres burned. (CNBC, 2019).

Figure 1 Study area location in Butte County, USA, and the distribution of fire scars (field plot distribution) within the study area. And (Landsat 8 OLI/TIRS C1 level 2 imagery: bands 7:5:4 as the R: G: B combination; Projection WGS 1984 UTM Zone 10N datum.

3 Data and methodology

This study is designed for identifying burn severity areas via the evaluation of spectral surface reflectance of the fire-affected regions and mapping the vegetation recovery, post-wildfire incident (10 months after). Available scenes from Landsat 8 OLI/TIRS C1 level 2 with < 10 percent cloud cover for September (pre-fire autumn 2018), January (just after the fire - Winter 2019), and September 2019 (post-fire autumn 2019 {recovery}), including paths 44 and row 32 and 33 were obtained from the USGS archive (Table 1). None of the scenes were preprocessed as it was ordered from USGS (custserv@usgs.gov) with additional criteria (preprocessing parameters) of land and scene cloud cover of less than 10 percent. All the concurrent products were visually inspected with particular attention to the burned localities and areas adjacent to that of the burns to affirm the elimination of contamination from clouds, shimmer, water, flaming fronts as well as bright, non-vegetated surfaces.

Table 3.1. List of Landsat 8 OLI/TIRS C1 level 2 with scenes obtained from USGS Customer Services Earth Resources Observation & Science Center (EROS).

Instruments	***Path***	***Row***	***Date***
OLI	44	33	September 21, 2018
OLI	44	33	January 27, 2019
OLI	44	32	September 24, 2019

Table 3.2. The Landsat OLI/TIRS Bands

Bands	**Wavelength (micrometers)**	**Resolution (meters)**
Band 1 - Coastal aerosol	0.43-0.45	30
Band 2 - Blue	0.45-0.51	30
Band 3 - Green	0.53-0.59	30

Band 4 - Red	0.64-0.67	30
Band 5 - Near Infrared (NIR)	0.85-0.88	30
Band 6 - SWIR 1	1.57-1.65	30
Band 7 - SWIR 2	2.11-2.29	30
Band 8 - Panchromatic	0.50-0.68	15
Band 9 - Cirrus	1.36-1.38	30
Band 10 - Thermal Infrared (TIRS) 1	10.6-11.19	100
Band 11 - Thermal Infrared (TIRS) 2	11.50-12.51	10

3.1 Burn severity mapping

Burn severity mapping current image processing software products provide an abundance of classification and analysis tools for digital data. Supervised and unsupervised classification of multispectral data is undoubtedly useful, given a broad category of landcover classification. As part of a trial and error process in the development of the methodology described here, several simple classification techniques were employed. These included Spectral transformation and thresholding and supervised classifications of Multi-spectral image (MSI) composed of band 7,6,4 and 3, and the classification of ratio and modified band da-ta. Our selected suite of spectral indices includes the normalize difference vegetation index (NDVI) (Tucker, 1979), and NBR. Each of the indexes presents some form of explanatory power in which two or more bands reveal changes in vegetation or other surface parameters, as can be expected after burning. The three indices assess the normalized differences between reflectance in NIR as the first component and red, SWIR 1.6, and SWIR 2.2 for NDVI, NDSWIR, and NBR, respectively.

3.2 Spectral Transformation and Thresholding

The NDVI and the NBR (Epting et al., 2005; Mallinis et al., 2018) are the two most common spectral indices used for burn intensity measurement (and local scale burned area estimates). These two spectral transformations were added to the OLI images, Normalized Burn Ratio Index(NBR) and the Normalized Difference Vegetation Index (NDVI) for September 21, 2018, January 27, 2019, and September 24, 2019. Key and Benson (2001) designed the NBR, also referred to as the Normalized Difference Infrared Index (Chuvieco et al., 2002), to distinguish burned and unburned areas and to quantify severe effects with a single index within the burns. The NIR (band 4) wavelengths are sensitive to the leaf structure of living vegetation, while the SWIR (band 7) is sensitive to moisture content and some soil conditions (Slaton et al., 2001).Table 1. Table 3.1. List of Landsat 8 OLI/TIRS C1 level 2 with scenes obtained from USGS Customer Services Earth Resources Observation & Science Center (EROS).

Vegetation influenced by flame exhibits reduced reflection of NIR and increased observation of SWIR. Usually, pre-and post-fire NBR is measured, and then the difference is determined to identify areas of significant change. The NBR (and difference NBR) was first used by Garcia and Caselles in 1991 to identify burned and unburned areas. Key and Benson later explored the ability of this index to determine varying degrees of burn severity within a heated area. Also, active measures of burn intensity can be determined by using NDVI and DNDVI data. However, NDVI is prone to variable outcomes at low canopy cover (Major er al., 1990; Huete et al., 1994)

and, therefore, may not be as useful for classifying burn severity across a variety of vegetation and soil conditions. These surface reflectance signatures and the de-rived spectral indices were subsequently used in the assessment of burn severity mapping capabilities from remotely-sensed data for the three dates individually.

3.3 Image Classification

3.3.1 Spectral Transform Input and Stacked Band

These were applied to the OLI/TIRS imagery. We selected a suite of spectral indices that are commonly used in characterizing surface parameters with relevance to burned area mapping. While this ensemble of the spectral index is not exhaustive, it is representative of various approaches to burned area mapping and combinatory capabilities of various Landsat bands. The spectral transformed image and the stacked image were classified using a supervised training approach and a maximum likelihood classifier. One hundred and thirty-five training sites were used in the monitored classification process. Thematic maps were produced for each combination of technique and study site (burnt and unburnt). In total, two detailed maps were produced (NBR image for the study site, and the supervised classification). A six-category classification scheme was tested for fire severity categories (“enhanced regrowth low,” “unburnt,” “low severity,” “moderate-low severity,” “moderate-high severity,” and “severe burn”) class.

Similarly, all unburnt areas around the scars were limited to areas that were known to be unburnt throughout the full time-span of the fire across the study area from November 8, 2018, to November 25, 2018, and were surrounded or immediately adjacent to the burns using visual analysis. All areas directly not affected were dropped from the analysis using the spatial masking technique. This spatial masking made it possible to avoid some of the typical confusion in digital classification between vegetation and non-vegetation categories. In total, we identified the following number of burned and unburned areas: 1) Burnt – 39749.6304 Unburnt, 10903.37942. This approach allowed us to obtain samples of burned and unburned regions for the scars using a consistent, replicable, and relatively unbiased approach with verification.

3.3.2 Vegetation Recovery

The NDVI index can be used to extract images of light, greenness, and health to access the level of vegetation recovery that has happened. The NDVI has been successfully used to identify vegetation and to provide a measure of its health and vitality. It has been positively correlated to measure such as leaf index and foilage protective cover. Brightness is sensitive to changes in soil reflectance of physical and biological influences (Crist and Cicone, 1984). Greenness is the sum of photosynthetic plant content (Patterson and Yool, 1998). Health is dependent on the difference between the visible bands (1–4) and the mid-infrared bands (5–7) and is prone to variations in plant moisture. The NDVI strength is that the Brightness, Greenness, and health coefficients can also be used to accentuate the scene characteristics of burned areas.

We calculated three separate NDVI values for September 21, 2018, January 27, 2019, and September 24, 2019, that were obtained based on band definitions for the Operational Land Imager (OLI) and Thermal Infrared Sensor (TIRS) imagery from the Landsat 8 satellite. These different values were utilized to obtain the Differenced Normalized Vegetation Index to compare the growth and change in vegetation of the area. The band definitions for OLI/TIRS NDVI were red = 640 - 670nm and near-infrared (NIR) = 2110 - 2290nm.

3.4 Single Date vs. Multi-temporal Inputs:

Vegetation recovery after a fire event is an important metric to determine better the long-term impact a fire had on an ecosystem. A multitude of factors determines the rate of recovery, including climate, initial plant mortality, soil characteristics, degree of soil disturbance, topographic influences, and vegetation composition. Both single-date and multi-temporal (i.e., pre- and post-fire dates) and (i.e., pre- and post-vegetation dates) of Landsat 8 OLI/TIRS data were performed to determine which provides a better delineation of the burn extent and offered additional information about the area of vegetation recovery respectively. The data improves the accuracy of the burn severity extent map. Because the NDVI and NBR helped with obtaining a better perception of the enhanced image for the study site in the testing of spectral transforms (as summarized in the Results section), it was used for the comparison of a single date and bi-temporal approaches.

To create the Burn ratio change image, referred to as the ΔNBR image, the pre-fire image was subtracted from the post-fire image. The single date and differenced (Δ)NBR went through a spectral transformation via thresholding. Thematic maps were produced and compared, for the study area and temporal characteristic (single date and differenced multi-temporal NBR) to enhance image interpretation. As earlier stated in the previous section, the method consists of first producing NDVI and NBR images for the three different periods obtained and then calculating their arithmetic difference. Next, a threshold of change (difference) was defined to separate change from no change. This method assumes that the difference of NDVIs across the entire study area follows a normal distribution and that the changes (atypical values) are in the tail of the distribution. Hence, change can be identified based on a threshold measured in standard deviation units from the global mean difference. This threshold was computed based on:

$$\text{Con("raster\_image"} < (\mu - k\sigma),-1,\text{Con("raster\_image"} > (\mu + k\sigma),1,0)) \quad (3)$$

Where raster_imagae = NDVI/NBR obtained raster image

k is a scalar that defines the number of standard deviation (σ) units from the mean (μ) considered to indicate change.

The United States Geological Survey (USGS) proposed a classification table to interpret the burn severity (dNBR), which can be seen in Table 3 below. In our data, the lowest value is -1.46, demonstrating that there were values related to detectable regrowth. A large number of ambiguous pixels (red) is caused by the two months difference between our pre- and post-fire images. Due to the winter, the area likely remains the same with no form of regeneration between these two dates producing higher NBR difference as severity burn.

Table 3.3: The United States Geological Survey (USGS) proposed a classification

Severity Level	dNBR Range (scaled by 10^3)	dNBR Range (not scaled)
Enhanced Regrowth, high (post-fire)	-500 to -251	-0.500 to -0.251
Enhanced Regrowth, low (post-fire)	-250 to -101	-0.250 to -0.101
Unburned	-100 to +99	-0.100 to +0.99
Low Severity	+100 to +269	+0.100 to +0.269
Moderate-low Severity	+270 to +439	+0.270 to +0.439
Miderate-high Severity	+440 to +659	+0.440 to +0.659
High Severity	+660 to +1300	+0.660 to +1.300

4.0 Results and Discussion

A combined approach was used in this study. The period covered by the map and the Indices utilized allowed for the combination of both datasets to investigate months before the wildfire, the fire period, and the first ten months of development following the wildfire. We used both NDVI, NBR, and Supervised classification to map burn area extent, to detect burn severity and highlight changes in green vegetation abundance. The time series analysis was conducted at burned area scale because it provides aggregated and statistically significant estimations of change for a large number of geographically defined pixels, such as latitude bands or ecological zones (Slayback et al., 2003).

The supervised classification enabled us to achieve the aim of delineating the boundary of the burn extent, which was also compared with the map produced from the NBR and NDVI (Figure 4.1 and figure 4.2). The area was classified into two classes: burnt area and unburnt area. The result of theNDVI, NBR and supervised classification are shown below.

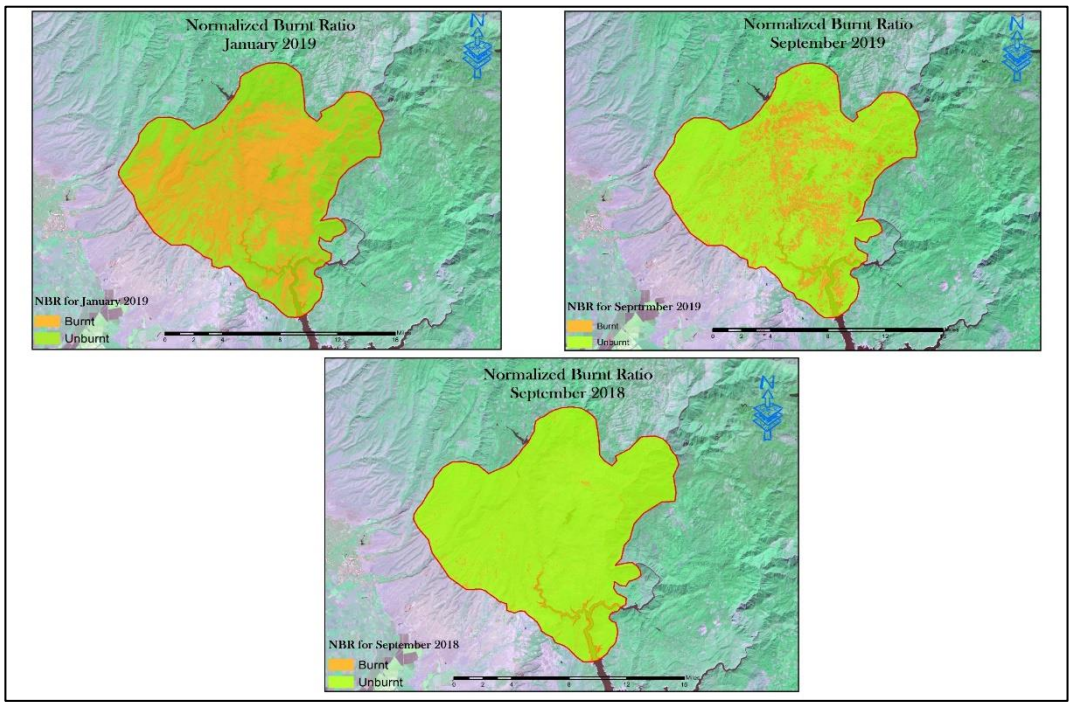

Figure 4.1. NBR index Map of Butte County (Promise City) for Landsat 8 OLI/TIRS

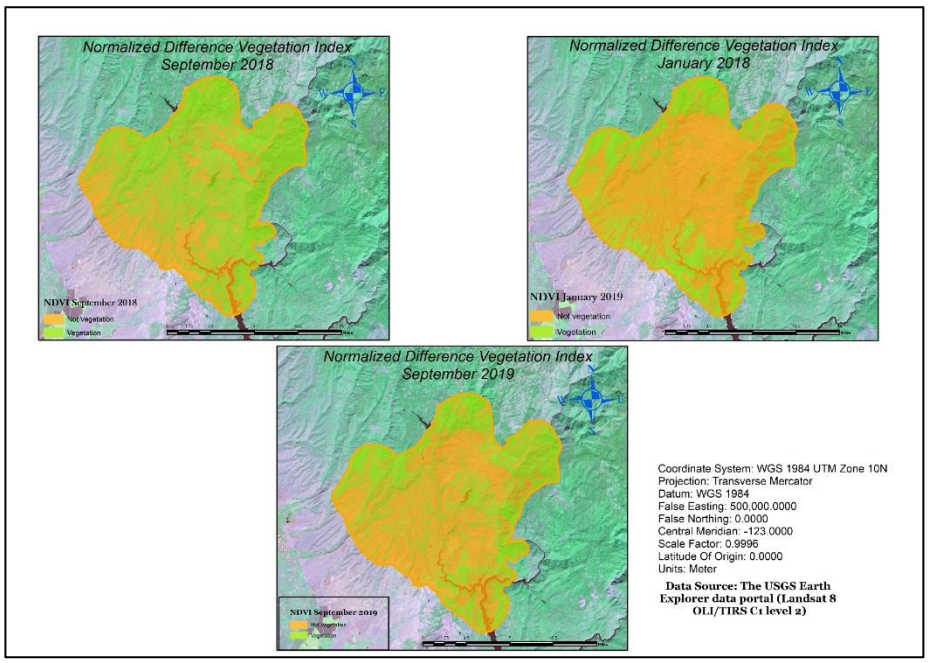

Figure 4.2. NDVI index Map of Butte County (Promise City) for Landsat 8 OLI/TIRS

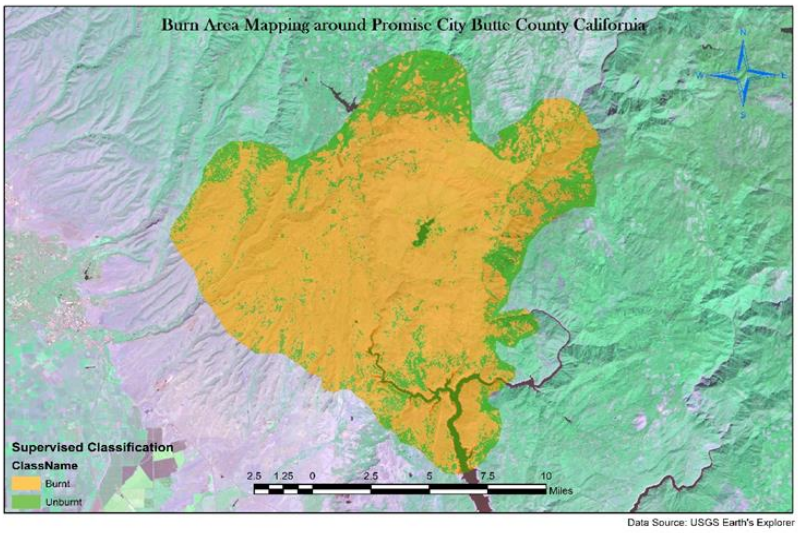

Figure 4.3. supervised classification Burn Map of Butte County (Promise City) for Landsat 8 OLI/TIRS

Table 4.1. It provides the overall accuracy obtained from producing the above map. The accuracy of the output was also compared with that produced using NDVI and NBR index. The Supervised classification analysis shows the smallest errors. In particular, the best production was achieved with the Maximum

Likelihood classifier (MLC) applied to the multispectral stacked image of band 7,5, and 4. We performed an overall accuracy of 86%, with 72% as kappa. Also, the confusion matrix of NDVI and the NBR index were computed after being utilized to delineate the burn area. This validation was compared with the result of the MLC to see which their different attitudes and characteristics in achieving the output. The overall accuracy obtained for NDVI and NBR was 78% and 62% respectively

Table 4.1.: User, Producer, and Overall efficiency obtained for Maximum Likelihood Classification, NDVI, and NBR.

OBJECTID	ClassValue	Burnt	Unburnt	Total	U_Accuracy (%)	Kappa
0	Burnt	23	6	29	79.31034	0
1	Unburnt	1	20	21	95.2381	0
2	Total	24	26	50	0	0
3	P_Accuracy (%)	95.83333	76.92308	0	86	0
4	Kappa	0	0	0	0	72.17806

Table 4.2: Overall, User and Producer accuracy obtained for NDVI for burn area delineation

OBJECTID	ClassValue	Burnt	Unburnt	Total	U_Accuracy (%)	Kappa
0	Burnt	31	2	33	93.93939394	0
1	Unburnt	9	8	17	47.05882353	0
2	Total	40	10	50	0	0
3	P_Accuracy (%)	77.5	80	0	78	0
4	Kappa	0	0	0	0	45.54455

Table 4.3: Overall, User and Producer accuracy for NBR

OBJECTID	ClassValue	Burnt	Unburnt	Total	U_Accuracy (%)	Kappa
0	Burnt	24	0	24	100	0
1	Unburnt	18	8	26	30.76923077	0
2	Total	42	8	50	0	0
3	P_Accuracy (%)	57.14285714	100	0	64	0
4	Kappa	0	0	0	0	29.90654206

Also, we produced a fire severity map for our study area based on the United States Geological Survey (USGS) proposed classification and compared this classification visually based on the degree of soil surface color alteration, i.e., reddening of soils due to iron oxide formation. The presence of iron-oxide in soils increases reflectance across the study area and is seen after the band stacking and contrast enhancement of the imagery. This fire severity was applied to the Differenced Normalized Burn Ratio (DNBR), figure 4.4. The separated NBR pre- and post-fire images result in a fire-related transition picture categorized into severity categories and provide an impartial framework for assessing potential fire effects (Eidenshink, 2007). Hence the DNBR was produced and classified based on the USGS classification scheme.

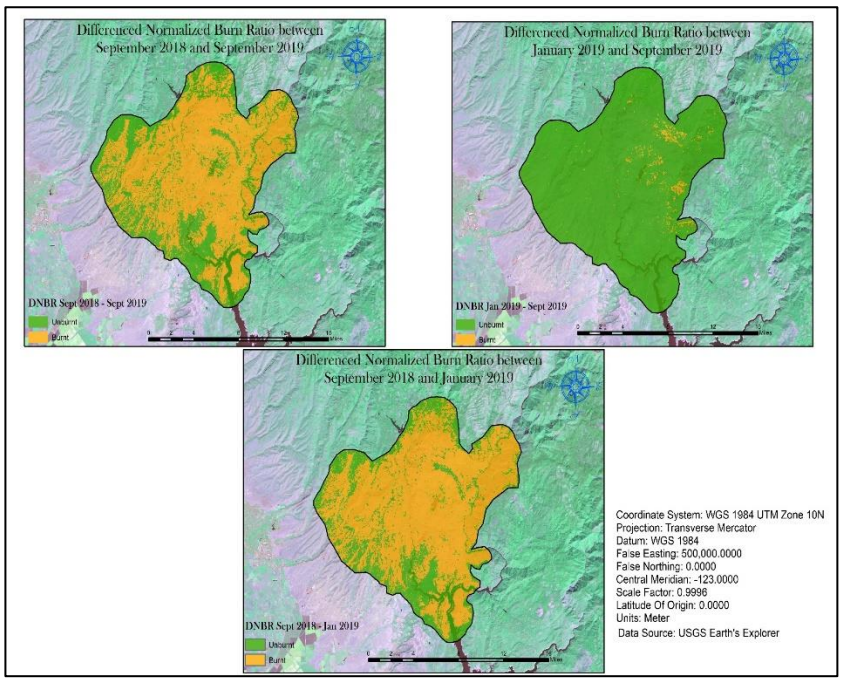

Figure 4.4. DNBR index Map of Butte County (Promise City) for Landsat 8 OLI/TIRS

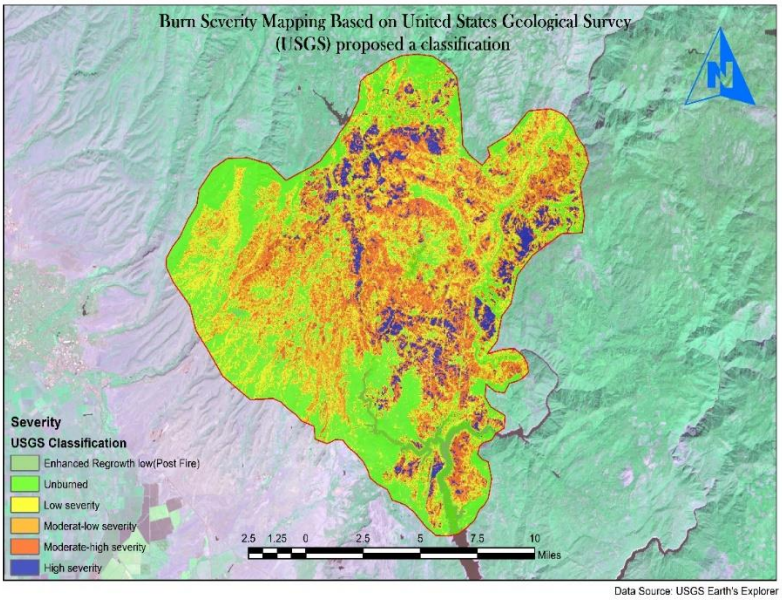

Figure 4.5. The Burn Severity Map for Butte County using Landsat 9 OLI and the USGS fire severity Classification

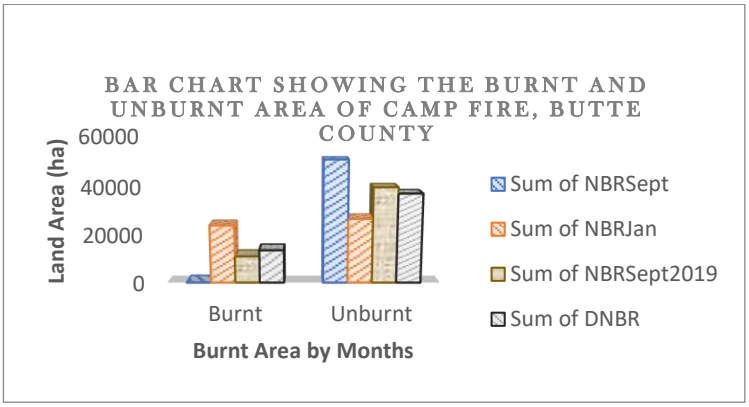

Figure 4.6. Graph showing the attitude of the piece of land as represented by NBR

Accessing Vegetation Recovery

The Vegetation recovery for the post fire was obtained using NDVI (refer to figure 4.2) and also obtained via the MLC classifier with the help of visual interpretation to capture the vegetation recovery map as well as the amount of vegetation cover at the different times over the study area. The result of classification analysis can be seen below:

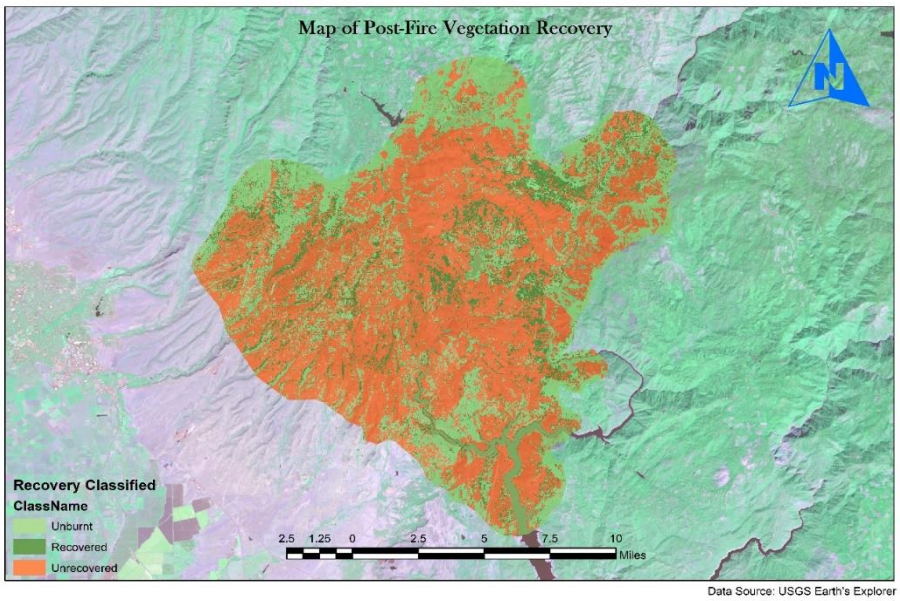

Figure 4.7. The Map of Post-fire Vegetation recovery using MLC

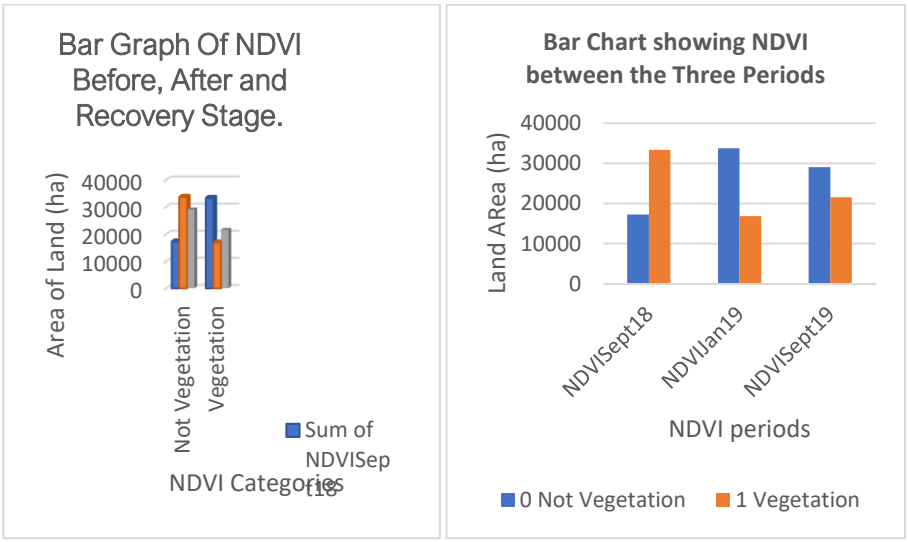

Figure 4.8: Comparison between the amount of Vegetation and nonvegetation

From Figure 4.2, 4.7 and 4.8 above, one can see that the vegetation at the topsoil (visual cognition) has started to recover especially towards the center. This output was validated by computing the confusion matrix, which obtained a total of 77.78% overall accuracy.

Table 4.4. Confusion Matrix of Vegetation recovery using MLC

OBJECTID	ClassValue	Unburnt	Recovered	Unrecovered	Total	U_Accuracy	Kappa
0	Unburnt	12	1	3	16	75	0
1	Recovered	0	2	8	10	20	0
2	Unrecovered	0	0	28	28	100	0
3	Total	12	3	39	54	0	0
4	P_Accuracy	100	66.66667	71.79487179	0	77.77777778	0
5	Kappa	0	0	0	0	0	59.55056

Also, the output obtained using DNDVI for the difference between post-fire and immediately after the fire occurrence, as well as the USGS classification scheme, was unfavorable to check for vegetation recovery. The Map produced while using DNDVI appeared over-generalized when the small threshold was applied and was oversampled while adjusting for the appropriate limit. Also, the USGS classification did not give a true reflection of what existed on the ground and hence was not helpful (see Appendix 1 and 2). Finally, the Computation was made to know the amount of vegetation that was recovered which is 8.86% of the area of land (3525.132102) as delineated using MLC. The table below shows the amount of recovery based on the method of delineation of the burn severity.

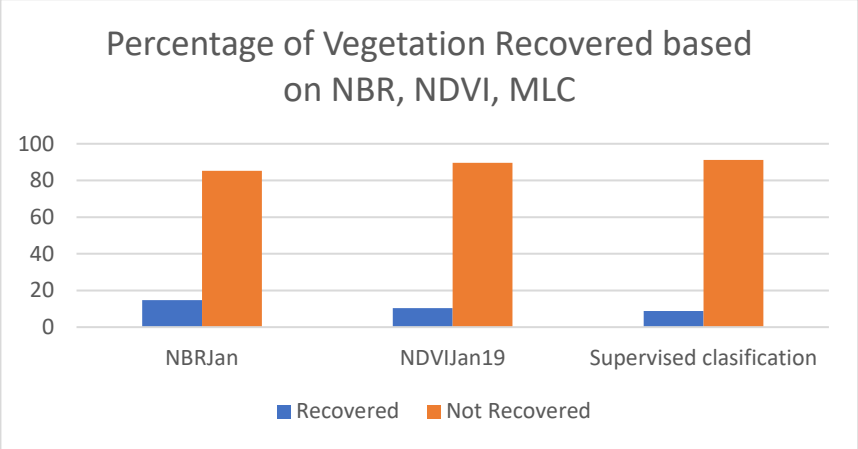

Conclusion

Mapping past fires and burn severity will facilitate scientists to recognize burning trends over time. The NBR index is calculated for pre- and post-fire images as described in the Methods. NBR images are differenced for each fire scene pair to generate the dNBR. As we have described previously, our burn severity mapping process was based on understanding what spectral bands were most sensitive to the fire. After checking other literature as well as after carrying out the whole process of the methodology, we found that the combination of band 7, band five and band 4 was susceptible to the characteristics of burn severity in the study area. Also, MLC was utilized and burn severity was created based on the USGS classification scheme. The NDVI data are also good indicators of burn severity. However, NDVI is subject to variable results at low canopy cover and, therefore, may not be as useful for classification of burn severity across a range of vegetation and soil conditions. Our results indicated that vegetation recovery has started. The best result was achieved when MLC and visual perception were applied. NDVI and NBR signal usually recover after a wildfire. At this time, many of the burned areas show NDVI values similar to the unburned control sites, while the NBR needs a more extended recovery period. The results also suggest that variability observed in postwildfire NDVI and NBR can be explained partially by the dominant land use type.

Further research will resolve some of the remaining uncertainties by introducing climate data, wildfire severity and latitude to the analysis since fire severity do not just affect vegetation but also settlements and human activities which is of utmost significance. When using the satellite images for the examination, 30m resolution is not sufficient because identifying the built-up area is quite tricky with that resolution. In the context of identifying land cover for an accurate analysis 30m, resolution satellite images are not suitable. The classification scheme presented here should apply to other forested burned areas. Landsat OLI bands 7,5 and 4 are equally sensitive to the appropriate burn severity parameters across a variety of wooded areas.

Acknowledgments

We would like to acknowledge our tutors Prof. Mario Caetano and Hugo Costa for the guidance and knowledge given throughout this project execution. We have learned to love remote sensing.

References

Bidoglio, G., De Plano, A., Avogadro, A., & Murray, C. N. (1984). Migration behavior and chemical

speciation of Np and Am under nuclear waste repository conditions. *Inorganica Chimica Acta*, *95*(1), 1–3. https://doi.org/10.1016/S0020-1693(00)85959-9

Chu, T., & Guo, X. (2013). Remote sensing techniques in monitoring post-fire effects and patterns of forest recovery in boreal forest regions: A review. *Remote Sensing*, *6*(1), 470–520. https://doi.org/10.3390/rs6010470

Crist, E. P., & Cicone, R. C. (1984). Application of the Tasseled Cap concept to simulated Thematic Mapper data. *Photogrammetric Engineering & Remote Sensing*, *50*(3), 343–352.

De Santis, A., & Chuvieco, E. (2007). Burn severity estimation from remotely sensed data: Performance of simulation versus empirical models. *Remote Sensing of Environment*, *108*(4), 422–435. https://doi.org/10.1016/j.rse.2006.11.022

Efthimiou, N., Psomiadis, E., & Panagos, P. (2019). Fire severity and soil erosion susceptibility mapping using multi-temporal Earth Observation data: The case of Mati fatal wildfire in Eastern Attica, Greece. *Catena*, (October), 104320. https://doi.org/https://doi.org/10.1016/j.catena.2019.104320

Eidenshink, J., Schwind, B., Brewer, K., Zhu, Z.-L., Quayle, B., & Howard, S. (2007). A Project for Monitoring Trends in Burn Severity. *Fire Ecology*, *3*(1), 3–21. https://doi.org/10.4996/fireecology.0301003

Epting, J., Verbyla, D., & Sorbel, B. (2005). Evaluation of remotely sensed indices for assessing burn severity in interior Alaska using Landsat TM and ETM+. *Remote Sensing of Environment*, *96*(3–4), 328–339. https://doi.org/10.1016/j.rse.2005.03.002

https://www.cnbc.com/2019/11/10/more-companies-are-flagging-wildfire-risk-as-suppression-costs-climb.html

Key, C. H., & Benson, N. C. (2006). Landscape Assessment (LA) sampling and analysis methods. *USDA Forest Service - General Technical Report RMRS-GTR*, (164 RMRS-GTR).

Mapping Habitats in Alpine Regions Using Multi-Temporal RapidEye Data. (2013). 536–539. https://doi.org/10.1553/giscience2013s536

Palacios, A., Chuvieco, E., & Martin, M. P. et al. (2002). Assessment of different spectral indices in the red-near-infrared spectral domain for burned land discrimination. *International Journal of Remote Sensing*, *23*(23), 5103–5110.

Patterson, M. W., & Yool, S. R. (1998). Mapping fire-induced vegetation mortality using landsat thematic mapper data: A comparison of linear transformation techniques. *Remote Sensing of Environment*, *65*(2), 132–142. https://doi.org/10.1016/S0034-4257(98)00018-2

Schneising, O., Buchwitz, M., Reuter, M., Bovensmann, H., & Burrows, J. P. (2019). Devastating Californian wildfires in November 2018 observed from space: the carbon monoxide perspective. *Atmospheric Chemistry and Physics Discussions*, (January), 1–14. https://doi.org/10.5194/acp-2019-5

Slaton, M. R., Hunt, E. R., & Smith, W. K. (2001). Estimating near-infrared leaf reflectance from leaf structural characteristics. *American Journal of Botany*, *88*(2), 278–284. https://doi.org/10.2307/2657019

Slayback, D. A., Pinzon, J. E., Los, S. O., & Tucker, C. J. (2003). Northern hemisphere photosynthetic trends 1982-99. *Global Change Biology*, *9*(1), 1–15. https://doi.org/10.1046/j.1365-2486.2003.00507.x

Tran, B. N., Tanase, M. A., Bennett, L. T., & Aponte, C. (2018). Evaluation of spectral indices for assessing fire severity in Australian temperate forests. *Remote Sensing*, *10*(11), 1–24. https://doi.org/10.3390/rs10111680

Tucker, C. J. (1979). Red and photographic infrared linear combinations for monitoring vegetation.

Remote Sensing of Environment, *8*(2), 127–150. https://doi.org/10.1016/0034-4257(79)90013-0

Veraverbeke, S., & Hook, S. J. (2013). Evaluating spectral indices and spectral mixture analysis for assessing fire severity, combustion completeness and carbon emissions. *International Journal of Wildland Fire*, *22*(5), 707–720. https://doi.org/10.1071/WF12168

Veraverbeke, S., Stavros, E. N., & Hook, S. J. (2014). Assessing fire severity using imaging spectroscopy data from the Airborne Visible/Infrared Imaging Spectrometer (AVIRIS) and comparison with multispectral capabilities. *Remote Sensing of Environment*, *154*, 153–163. https://doi.org/10.1016/j.rse.2014.08.019

Viana-Soto, A., Aguado, I., & Martínez, S. (2017). Assessment of Post-Fire Vegetation Recovery Using Fire Severity and Geographical Data in the Mediterranean Region (Spain). *Environments*, *4*(4), 90. https://doi.org/10.3390/environments4040090

Wasser, L & Cattau, M. Work with the Difference Normalized Burn Index - Using Spectral Remote Sensing to Understand the Impacts of Fire on the Landscape.